PCCP

Surface Behavior of Amphiphiles in Aqueous Solution: A Comparison between Different Pentanol Isomers

Journal:	*Physical Chemistry Chemical Physics*
Manuscript ID:	CP-ART-03-2015-001870.R1
Article Type:	Paper
Date Submitted by the Author:	29-Apr-2015

Complete List of Authors:	Walz, Marie-Madeleine; Uppsala University, Department of Physics and Astronomy Caleman, Carl; Uppsala University, Department of Physics and Astronomy; DESY, Center for Free-electron Laser Science Werner, Josephina; Uppsala University, Department of Physics and Astronomy; Swedish University of Agricultural Sciences, Department of Chemistry and Biotechnology Ekholm, Victor; Uppsala University, Department of Physics and Astronomy Lundberg, Daniel; Swedish University of Agricultural Sciences, Department of Chemistry and Biotechnology Prisle, Nønne; Helsinki University, Department of Physics Öhrwall, Gunnar; Lund University, MAX IV Laboratory Björneholm, Olle; Uppsala University, Department of Physics and Astronomy

Journal Name

RSCPublishing

ARTICLE

Surface Behavior of Amphiphiles in Aqueous Solution: A Comparison between Different Pentanol Isomers

Cite this: DOI: 10.1039/xoxxoooooox

Received ooth January 2012,
Accepted ooth January 2012

DOI: 10.1039/xoxxoooooox

www.rsc.org/

M.-M. Walz[a], C. Caleman[a,b], J. Werner[a,c], V. Ekholm[a], D. Lundberg[c], N. L. Prisle[d], G. Öhrwall[e], and O. Björneholm[a]

Position isomerism is ubiquitous in atmospheric oxidation reactions. Therefore, we compare surface-active oxygenated amphiphilic isomers (1- and 3-pentanol) at the aqueous surface with surface- and chemically sensitive X-ray photoelectron spectroscopy (XPS), which reveals information about the surface structure on a molecular level. The experimental data is complemented with molecular dynamics (MD) simulations. A concentration-dependent orientation and solvation of the amphiphiles at the aqueous surface is observed. At bulk concentrations as low as around 100 mM, a monolayer starts to form for both isomers, with the hydroxyl groups pointing towards the bulk water and the alkyl chains pointing towards the vacuum. The monolayer (ML) packing density of 3-pentanol is approx. 70 % of the one observed for 1-pentanol, with a molar surface concentration that is approx. 90 times higher than the bulk concentration for both molecules. The molecular area at ML coverage (≈ 100 mM) was calculated to be around 32 ± 2 Å^2/molecule for 1-pentanol and around 46 ± 2 Å^2/molecule for 3-pentanol, which results in a higher surface concentration (molecules/cm^2) for the linear isomer. In general we conclude therefore that isomers – with comparable surface activities – that have smaller molecular areas will be more abundant at the interface in comparison to isomers with larger molecular areas, which might be of crucial importance for the understanding of key properties of aerosols, such as evaporation and uptake capabilities as well as their reactivity.

1 Introduction

In atmospheric science the surface structure of water is of particular interest as it plays a key role in many interfacial processes.[1] One example in this context is atmospheric aerosols, relevant for the global radiation budget and cloud formation. Aerosol effects are still the major uncertainty in the total radiative forcing estimates, which are crucial to predict climate changes.[2] These airborne solid and liquid particles have a size distribution in the nanometer to micrometer range, which results in a high surface-to-bulk ratio. Therefore, the surface and its chemical composition determine the physico-chemical interface properties of the aerosols. A precise molecular level understanding of the surface properties may be vital to the understanding of aerosol effects, as discussed earlier in more detail.[3] Aerosols originating from the surfaces of seas and lakes contain a significant amount of organic material in addition to inorganic components.[4] As bubbles at the water surfaces burst upon wave action, they create a fine spray of droplets, whose content is determined by that of the surface.[5] Surface-active organic compounds tend to accumulate at the water-vapor interface, which may alter the properties of the surface, e.g. lower the surface tension. Thus, chemistry occurring on the surface of aerosol droplets is affected by the organic content, and the behavior of the organic molecules at the droplet-air interface.[6] To understand this on a molecular level is crucial, as the surface structure may influence the physico-chemical properties of the interface,[3,7] such as evaporation and condensation, thereby affecting e.g. cloud formation and chemical reactivity of aerosols.[8,9] Thus, a better understanding of the surface structure of the interface may provide valuable information to improve existing climate models.

The content of organic compounds in aerosols and cloud droplets has been observed to vary from 20 to up to 90 wt%.[10] In tropospheric aerosols a large fraction of them are surface-active short-chained oxygenated compounds.[11] As an example for such compounds we studied pentanol, and compare two of its positional isomers. Position isomerism is ubiquitous in atmospheric oxidation reactions,[12] and such isomers can have very different physical and chemical properties,[13] thus it is of interest to understand their impact on the surface structure. Furthermore, the surface structure of short-chained alcohols in aqueous solution in general is not yet well understood.[9,14] The newly found extremely low-volatility organic compounds, ELVOCs, which are hypothesized to make a crucial

contribution to the "missing secondary organic aerosol" mystery,[15] are also believed to contain significant alcohol functionality, as are humic-like substances (HULIS)[16]. It is therefore of interest to gain more knowledge on the impact of alcohol functional groups at the water-vapor interface. These highly complex molecules are however too difficult to study immediately. Simpler alcohols, such as pentanol, provide a valuable intermediate step here, as their spectra are easier to interpret, and samples better handled, and much better constrained in terms of other properties, such as solubility, vapor pressure, and surface activity.

The two amphiphilic positional isomers, 1- and 3-pentanol, at the aqueous surface were studied with surface- and chemically sensitive soft X-ray photoelectron spectroscopy (XPS) and molecular dynamics (MD) simulations. XPS, which is commonly applied in solid-state physics, is not only elemental sensitive but also sensitive to the formal oxidation state of an atom and its local chemical and physical environment, i.e. in this study to the interaction of the pentanol with water and other pentanol molecules. This information is reflected in the binding energy and intensity of the core-level photoelectrons. MD simulations have been used to interpret and support the experimental findings, providing a deeper insight in the surface behavior of the studied molecules.

2 Experimental

X-ray photoelectron spectroscopy measurements

All XPS measurements were performed at MAX IV Laboratory, Lund, Sweden[17] at the I411 undulator beamline. To perform XPS at the water-vapor interface, a liquid micro-jet set-up was utilized. Details on this technique can be found e.g. in reference [18]. The liquid micro-jet (Ø ≈ 20 µm, flow rate ≈ 0.5 ml/min, T ≈ 283 K) is injected through a glass nozzle into an evacuated analysis chamber. Photoionization by linearly polarized synchrotron radiation occurs at approx. 1 mm behind the injection point, before the liquid jet breaks up into droplets and is frozen out in a cold trap. The photoelectrons are detected by a hemispherical electron energy analyzer (Scienta R4000) mounted perpendicular to the propagation direction of the liquid jet, at 54.7° ("magic angle") relative to the polarization plane of the synchrotron light to minimize angular distribution effects.[19] The total experimental resolution at the applied photon energy, E_{Photon} = 360 eV, is lower than 0.3 eV, as determined from the width of the water gas phase valence band $1b_1$ state. All spectra were energy calibrated against the binding energy of the $1b_1$ state (HOMO) of liquid water ($E_B(1b_1, \text{liquid})$ = 11.16 eV[20]) and intensity-normalized (against photon flux and acquisition time). To compare different experimental runs and to monitor the stability of the measurements, the $1b_1$ valence band state of liquid water of an aqueous sodium chloride solution (50 mM) was measured between all alcohol solutions and used as an internal intensity reference. The intensities of these reference measurements are constant within ± 5 – 10 %.

Aqueous solutions of 1-pentanol (≥ 99 %, Sigma-Aldrich) and 3-pentanol (98 %, Sigma-Aldrich) were prepared from de-ionized water (Millipore Direct-Q, resistivity > 18.2 MΩ cm) with concentrations in the range of $c_{1\text{-pentanol}}$ = 1.5–200 mM (mmol/l) and $c_{3\text{-pentanol}}$ = 12.5–500 mM. The solubility of 1-pentanol is approx. 300 mM and the one of 3-pentanol approx. 830 mM, both at 283 K.[21] To avoid charging of the liquid jet due to photoionization and electrokinetic charging all solutions contain 25 mM sodium chloride.[22]

The pentanol molecules at the interface were monitored via the C 1s signal using E_{Photon} = 360 eV. At this photon energy, the C 1s photoelectrons have a kinetic energy of approx. 70 eV, making the XPS measurements highly surface-sensitive,[19] as the effective attenuation length is estimated to be in the order of 1 nm.[23] The photoelectron spectra were fitted using least-squares method, using two symmetric Voigt line profiles for the liquid phase signal and four asymmetric PCI[24] line profiles for the gas phase signal for the respective pentanol molecule. The lifetime width for C 1s core-holes corresponding to the Lorentzian width was set to 0.1 eV.[25] Gaussian widths were free parameters, but linked such that they were the same for the corresponding peaks in all spectra. Energy positions and intensities were also free parameters. The contributing gas phase signal of the pentanol was fitted by linking the energy splitting and the intensity ratio to its 'pure' gas phase spectrum.

Molecular dynamics simulations

The MD simulations were performed using the GROMACS suite of programs.[26] To be able to exclude that the simulation results were force field dependent, all simulations were done using both the OPLS/AA force field[27,28] in combination with the SPC water model[29] and the generalized Amber force field (GAFF) in combination with the TIP3P water model.[28] Both these combinations of force fields and water models have been shown to reproduce Gibbs energies of hydration well and we therefore assume that they have reasonable surface properties.[30] Topologies (both GAFF and OPLS/AA) and molecular structures of the pentanol molecules were downloaded from the GROMACS Molecular & Liquid database available at http://virtualchemistry.org.[31] For further evaluation of the models and description of the procedure used to generate the topologies we refer to the literature.[32]

To generate the simulation boxes, one alcohol molecule (1-pentanol or 3-pentanol) was solvated in a box of water. The size of the initial water box was chosen such that we could build up the full simulation system by stacking the initial box into a 6 x 6 x 6 nm^3 box. Finally an empty 6 x 6 x 12 nm^3 box was added to generate a liquid-vacuum interface. The final simulation boxes contained water and 16 or 432 pentanol molecules. In the text where the simulation results are discussed, this is denoted as low and high concentration, respectively. 16 pentanol in the 216 nm^3 liquid slab corresponds to a system where only very few pentanol molecules reside at the surface. 432 pentanol molecules, on the other hand, generate a system with a partial monolayer (ML) on the surface (see Fig. 3 for illustration of the surfaces). A 2 ns equilibration simulation was performed on the system before the final 1 ns production run. To ensure that the systems had reached equilibrium the total energy of the equilibration run was monitored. Following in the procedures worked out in earlier simulations of water alcohol mixtures,[33,34] a 1.1 nm cutoff was used for both the Lennard-Jones interactions and the switching distance for the particle mesh Ewald (PME) algorithm for the Coulomb interactions.[35] The OPLS/AA force field was not developed to be used with PME, but extensive studies on organic macromolecules in water[36] showed that agreement of simulation results with experimental data improves when long-range interactions are taken into account explicitly, independent on choice of force field. The temperature in the simulations were set to 283 K, and was kept at this level using the Berendsen temperature coupling algorithm, and a coupling constant of 0.1 ps.[37] In all simulations, the bonds were constrained using the LINCS algorithm,[38] and periodic boundary conditions were applied.

To calculate the radial distribution function (RDF) exclusively for the alcohol molecules on the surface, we had to do the analysis in several steps. First, the simulation trajectories were divided into 25 ps parts. For each of these parts of the trajectory, the water density along the axis perpendicular (the z-axis) to the water surface was calculated. Then, the surface was defined to be where the density changed from below 10 kg/m^3 to above. This gave us an average position of the surface for each 25 ps part. A pentanol molecule was considered to be "on the surface" if its oxygen atom was within 0.5 nm distance from the surface. In this way, we could define the surface for each 25 ps part of the trajectory separately, and calculate the RDF only for those. Finally an average RDF for the full simulation was calculated.

3 Results and discussion

In Fig. 1 the C 1s XPS spectra of 1-pentanol in aqueous solution for two concentrations (7.5 mM, solid line (intensity × 7.7) and 90 mM, dotted line) are depicted with their corresponding fits of the liquid phase signal. The fits of the respective gas phase signal are not depicted. The peaks at lower binding energies (below 290 eV) originate from the carbon atoms C2 – C5 of the alkyl chain, called "alkyl carbons" (C_C). The peaks at higher binding energies (above 291 eV) can be assigned to the carbon atom C1 to which the hydroxyl group is directly attached, here called "hydroxyl carbon" (C_{OH}). The higher electron binding energy of C_{OH} 1s compared to C_C 1s is due to a reduced electron density at the C_{OH} as the attached hydroxyl group is electron-withdrawing. The decreased shielding of the nucleus causes the C_{OH} 1s electrons to be more tightly bound. The C 1s signal from aqueous pentanol is shifted to lower binding energies (by roughly 0.6 eV) compared to the corresponding signal from gas phase molecules. The gas phase signal can be observed e.g. in the C 1s spectrum of the 90 mM 1-pentanol solution as a small shoulder towards higher binding energies. The lower binding energies of the dissolved molecules are primarily due to polarization screening of the charged C 1s core-hole final state by the solvent molecules.[39] The intensity of the 7.5 mM C 1s spectrum has been scaled (with a factor of 7.7) so that the C_{OH} 1s signals in both spectra match each other in order to clarify concentration-dependent changes in the spectral shape.

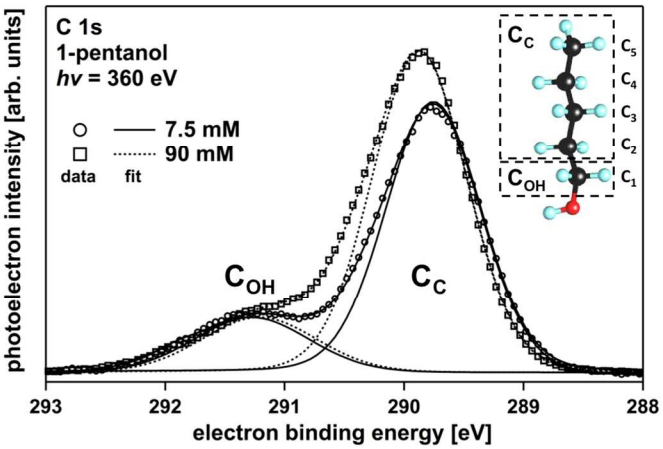

Fig. 1 C 1s XPS spectra of 1-pentanol in aqueous solution for two concentrations (7.5 mM, solid line (intensity × 7.7) and 90 mM, dotted line), acquired with a photon energy of E_{Photon} = 360 eV, shown with the respective fit of the liquid phase signal (C_C and C_{OH}). The fit for the gas phase is not shown.

Comparing the two spectra in Fig. 1, one can notice that besides the higher total intensity at higher concentration, the binding energies shift and the photoelectron (PE) intensity ratio R of the two peaks (C_C and C_{OH}) changes. While for 7.5 mM the C_C signal peaks at E_B = 289.75 ± 0.05 eV and the C_{OH} signal arises at E_B = 291.28 ± 0.05 eV, for 90 mM the respective signals are shifted to higher ($E_B(C_C)$ = 289.87 ± 0.05 eV) and slightly lower ($E_B(C_{OH})$ = 291.21 ± 0.05 eV) binding energy, respectively, thus the energy splitting ΔE_B between the C_C and C_{OH} signal decreases with increasing concentration (ΔE_B(7.5 mM) = 1.53 eV; ΔE_B(90 mM) = 1.34 eV). It should be noted that all determined ΔE_B values are independent of the E_B calibration (see *Experimental*), and thus more reliable and accurate than the absolute E_B values. Considering the PE intensity ratio R between the C_C and the C_{OH} peak areas, an increase is observed with concentration (R(7.5 mM) = 4.1; R(90 mM) = 4.9), meaning that the C_C signal increases relatively to the C_{OH} signal for higher concentration.

To elucidate this behavior further, a concentration-dependent study was conducted and all acquired spectra were evaluated regarding the total area A_{tot} of the liquid phase C 1s PE signal ($A_{tot} = A(C_C) + A(C_{OH})$), the ratio R between the two liquid phase C 1s peak areas ($R = A(C_C) / A(C_{OH})$) and the PE binding energy splitting ($\Delta E_B = E_B(C_{OH}) - E_B(C_C)$). To gain a deeper understanding on how different amphiphilic positional isomers act at the aqueous surface, 1- and 3-pentanol were compared. These isomers have the same molecular formula, $C_5H_{11}OH$, but differ in their connectivity. In 1-pentanol, the hydroxyl group (-OH) is attached to a terminal carbon atom of the alkyl chain (primary alcohol), whereas in 3-pentanol it is bonded to the middle carbon atom (secondary alcohol). The C 1s XPS spectra of aqueous 3-pentanol solutions overall show the same spectral features as the spectra of the aqueous 1-pentanol solutions that are shown in Fig.1, i.e. there are two peaks that can be assigned to the alkyl carbons and the hydroxyl carbon, respectively (see *Supporting Information Fig. S1*).

The results of the concentration-dependent study for 1- and 3-pentanol are depicted in Fig. 2. The y-axis is in Fig. 2a the total area A_{tot}, in Fig. 2b the ratio R, and in Fig. 2c the binding energy splitting ΔE_B. The x-axis in all plots is the molar concentration c of pentanol in aqueous solution.

Surface coverage

The trend of the total PE signal of pentanol with increasing concentration (see Fig. 2a) is comparable for both isomers and resembles a Langmuir adsorption isotherm.[40] It can be divided into two regions based on the change in the slope of the curves. In the first region (0 < c < 100 mM) the PE signal increases linearly with concentration, whereas in the second region (c ≥ 100 mM), no further significant increase of the PE intensity is observed, i.e. A_{tot} saturates. Due to the short effective attenuation length of the photoelectrons, the PE signal primarily originates from within a few nm of the surface and is thus strongly dependent on the concentration of molecules at the interface. If XPS was completely bulk-sensitive (as this is the case for photoelectrons with much higher kinetic energies), the PE intensity would scale linearly with the bulk concentration, independent from what occurs on the surface. Likewise, surface-sensitive XPS could show a linear increase in the PE signal if the surface concentration is changed in the same way as the bulk concentration. From this we can conclude that the shape of the Langmuir-like curve (as shown in Fig. 2a) results

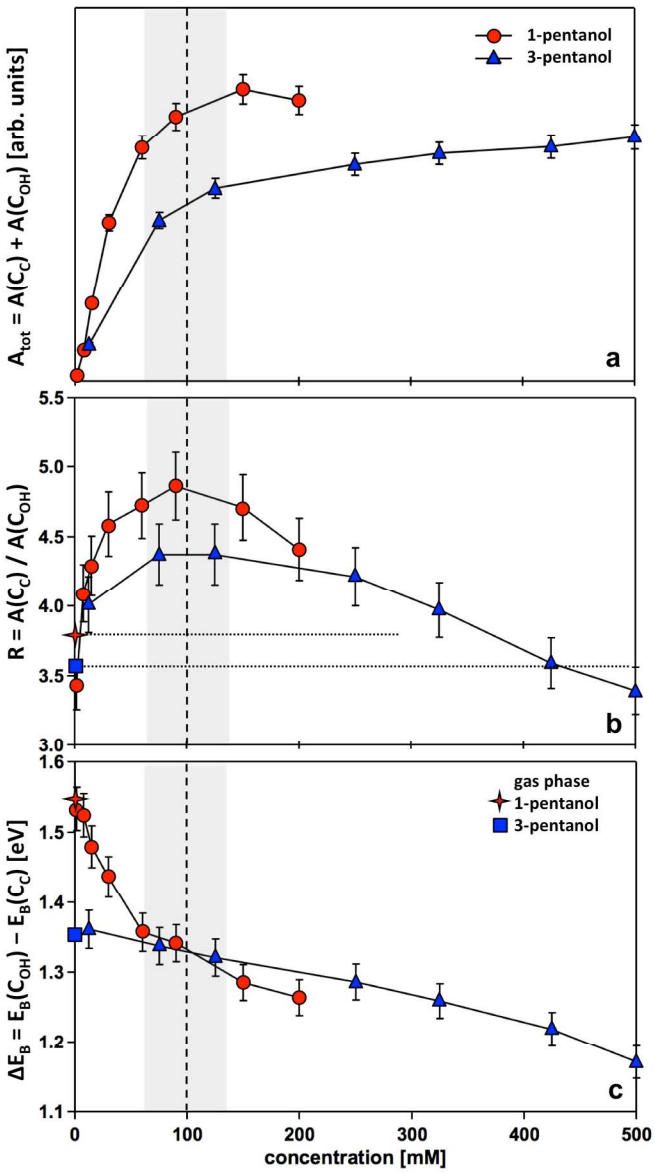

Fig. 2 Results of the C 1s XPS spectra of 1- and 3-pentanol at different concentrations: (a) total area of the liquid phase C 1s PE signal (A_{tot}), (b) PE intensity ratio between the liquid phase C_C and C_{OH} signal areas (R), and (c) electron binding energy splitting (ΔE_B); R and ΔE_B for the gas phase is indicated at c = 0 mM. The dashed line corresponds to c_{ML}, the grey area indicates that this is not a sharp transition.

from the saturation of the surface coverage, i.e. the adsorption of the amphiphiles at the aqueous surface with increasing bulk concentration and finally the formation of a monolayer at $c_{ML} \approx$ 100 mM. In Fig. 2, a dashed line indicates c_{ML}. The grey area around the dashed line indicates that a monolayer on a liquid surface is in dynamic equilibrium with the bulk and the gas phase, and may occur in a certain concentration range resulting in monolayers with different packing densities depending on e.g. the exact orientation and conformation of the adsorbing molecules. For 3-pentanol, a slight linear increase of the PE signal above 100 mM is observed, which is suggested to originate from pentanol molecules in the surface-near-bulk

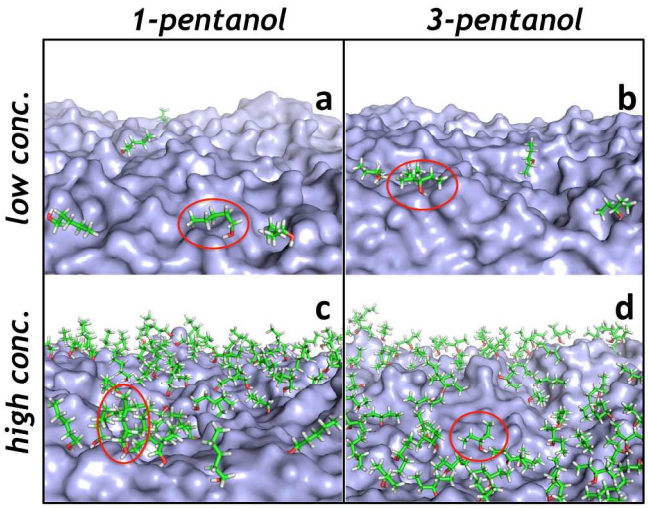

Fig. 3 Results from the MD simulations in "bird's eye view" for 1- and 3-pentanol at the aqueous surface at low (a, b) and high (c, d) concentration / surface coverage.

region where the concentration increases further after ML formation. It is observed that A_{tot} of 1-pentanol is higher for all concentrations than the corresponding signal for 3-pentanol, and furthermore, that the ML forms already at $c_{ML} \approx$ 100 mM for both isomers, although this is well below their solubility limit (around 300 mM for 1-pentanol and 830 mM for 3-pentanol at 283 K[21]), which is discussed in more detail later.

Orientation of the molecules at the interface

Two regions are also observed when evaluating the PE intensity ratio R between the two C 1s peak areas, i.e. $A(C_C)$ / $A(C_{OH})$ (see Fig. 2b). First, R increases up to approx. 100 mM, then it decreases for c > 100 mM. These two regions coincide with the ones observed for the Langmuir-like intensity curve. In the first region, R increases from around 4 until a ML is formed: up to 4.9 (100 mM) for 1-pentanol and up to 4.4 (100 mM) for 3-pentanol. At higher concentrations it decreases for 1-pentanol to 4.4 (200 mM) and for 3-pentanol to 3.4 (500 mM). Note that the exact values depend on the applied fitting procedure, while the general trend is always observed.

Assuming that the photoionization cross-section of C_C and C_{OH} is approximately the same,[41] and that the amphiphiles are randomly oriented, one expects a ratio for pentanol that is close to its stoichiometric ratio, i.e. 4 (4:1). The gas phase values have been determined to be around 3.6 for 3-pentanol and 3.8 for 1-pentanol, which is slightly lower than the ideal, stoichiometric value. A deviation from this ratio indicates that the amphiphiles have a preferential orientation at the aqueous surface. The observed ratio for 0 < c < 100 mM which increases with concentration, indicates thus that the signal from the C_{OH} is progressively dampened as the molecules gradually "stand up". The results from the MD simulations of 1- and 3-pentanol at the aqueous surface are depicted in Fig. 3 for low (3a and b) and high (3c and d) surface coverage (see *Simulations*) and are compared to the results from Fig. 2b.

At very low concentrations, where the pentanol molecules interact mainly with water at the aqueous surface, the alkyl chain of the pentanol molecules are oriented "parallel" to the aqueous surface (Fig. 3a and b), which is in line with the experimentally observed ratio that is close to 4, i.e. all carbon atoms contribute equally to the acquired C 1s signal. At higher

concentrations, more and more amphiphilic molecules accumulate at the aqueous surface and interact with each other. At surface coverage close to a ML (Fig. 3c and d), the amphiphilic molecules have a preferential orientation such that the hydrophilic hydroxyl groups point towards the bulk water, while the hydrophobic alkyl chains point towards the vacuum. In this orientation, the alkyl chain C 1s signal is enhanced and the hydroxyl carbon signal is dampened, resulting in R > 4. This preferential orientation of the amphiphilic molecules is proposed to be driven by hydrophobic / hydrophilic interactions of the amphiphiles with the solvent water and by van der Waals interactions between the alkyl chains.

If one compares 1- and 3-pentanol at ML coverage, a higher ratio R (i.e. 4.9 vs. 4.4), is observed for 1-pentanol. The larger ratio for 1-pentanol indicates a stronger dampening of the C_{OH} 1s PE signal. In a densely packed ML, where the hydroxyl groups are oriented towards the bulk water and the alkyl chains point towards the vacuum, it is obvious that the C 1s signal from C_{OH} is dampened more for a primary alcohol with a longer alkyl chain (all-trans length approx. 0.5 nm[42]) than for a secondary alcohol with two shorter ones (length approx. 0.3 nm[43]), qualitatively explaining the observed R_{ML}(1-pentanol) > R_{ML}(3-pentanol).

At concentrations higher than 100 mM, R decreases for both isomers. It is suggested that this decline can be explained by the contributing surface-near-bulk signal (explained in more detail in the next section). At any concentration the PE signal is comprised of contributions from the surface ($I_{surface}$) and the bulk (I_{bulk}). Thus, the experimentally determined ratio R is comprised of the two different ratios, $R_{surface}$ and R_{bulk}, which are weighted by the PE signal originating from the surface and bulk, and can be expressed as follows $R = [(I_{surface} \times R_{surface}) + (I_{bulk} \times R_{bulk})] / (I_{surface} + I_{bulk})$. $R_{surface}$ is dependent on the surface coverage, while R_{bulk} is constant at ≈ 4. In the first region (0 < c < 100 mM), $R_{surface}$ and the number of molecules accumulating at the interface (i.e. $I_{surface}$) increases with concentration causing R to increase. In the second region (c ≥ 100 mM) $I_{surface}$ and $R_{surface}$ stay constant as a ML has already formed. However, the bulk PE signal I_{bulk} (with R_{bulk} ≈ 4) increases further after a ML is formed, explaining why the total ratio R drops.

Surface concentration and molecular area at ML coverage

The higher total PE signal A_{tot} for 1-pentanol at any concentration indicates that there are more 1-pentanol molecules than 3-pentanol molecules at the interface, i.e. at ML coverage a higher surface packing density of the primary alcohol, as the PE signal is strongly dependent on the concentration of molecules at the aqueous surface and two isomers are compared. The higher surface concentration of 1-pentanol correlates with lower solubility in water compared to 3-pentanol (see *Experimental*). At c_{ML} the A_{tot} of 1-pentanol is approx. 50 % higher than the one measured for 3-pentanol. The lower packing density of 3-pentanol compared to the linear isomer 1-pentanol is not unreasonable considering steric hindrance: the two shorter alkyl chains require more space than the one linear alkyl chain (in all-trans conformation). This phenomenon has been observed earlier for other isomers of heptanol to dodecanol in a study in which vibrational sum frequency generation spectroscopy and surface tension measurements were combined.[44] This study suggests that linear alcohols form monolayers with alkyl chains in all-trans conformation aligned with the surface normal, resulting in very little conformational disorder, while 2- and 3-position isomers do not pack as efficiently in a monolayer but instead adopt structures with gauche defects.

As the intensity of the PE signal decreases according to an exponential decay function with increasing probing depth, approximately 95 % of the PE signal originates from within three times the effective attenuation length (EAL, λ), i.e. 3λ. At a kinetic energy of the photoelectrons of approx. 70 eV, the EAL in water is in the order of magnitude of λ ≈ 1 nm,[23] which means that 95 % of the PE signal originates from within approx. 3 nm.

If a ML is formed, it has a thickness of approx. 0.6 nm[42] for 1-pentanol (all-trans conformation) and around 0.4 nm[43] for 3-pentanol (with a conformation where the alkyl chains point towards the vacuum), respectively, corresponding to the molecular lengths. Thus, approx. 40 % (1-pentanol) and 30 % (3-pentanol) of the total PE signal originates from the ML at the surface, assuming λ ≈ 1 nm; the residual signal stems from the surface-near-bulk region. One should note that the organic molecules are strongly surface enriched, i.e. they have a much higher concentration at the interface compared to the surface-near-bulk region, which means that the acquired C 1s signal mainly stems from the molecules at the surface.

Knowing the ratio between the bulk and surface signal, the total measured PE signal can be used to estimate the surface enrichment factor $g = c_{surface} / c_{bulk}$, with $c_{surface}$ being the molar surface concentration and c_{bulk} being the bulk concentration.[45] The bulk signal was approximated by means of a reference measurement on a 0.5 M sodium formate solution.[3] At ML coverage (c_{ML} ≈ 100 mM) the surface enrichment factor was determined to be around $g = 86 \pm 5$ for both 1- and 3-pentanol.

The corresponding molecular area was calculated to be around 32 ± 2 Å^2/molecule for 1-pentanol and around 46 ± 2 Å^2/molecule for 3-pentanol, which is equal to a surface concentration of around $3.1 \times 10^{+14}$ molecules/cm^2 (or approx. 5.2×10^{-6} mol/m^2) for 1-pentanol and around $2.1 \times 10^{+14}$ molecules/cm^2 (or approx. 3.5×10^{-6} mol/m^2) for 3-pentanol. These values are in very good agreement with molecular areas and surface concentrations that have been reported for other alcohols in literature[44,46] and thus prove that XPS is a reliable experimental technique to determine such values. The resulting packing density of 3-pentanol is from these values approx. 68 % of the one of 1-pentanol. Due to the strong surface enrichment of the here investigated alcohol isomers, the formation of a ML is already observed around 100 mM, even though this is well below their solubility limit.

It should be noted that the molecular layer at the interface is not "plane" (see Fig. 3). As evaluated from the MD simulations molecular density plots of the alcohols and the water at the interface, the surface corrugation of the aqueous surface is in the order of 0.8 – 1.0 nm, and thus larger than the molecular dimensions (for further details see *Supporting Information Fig. S2*).

Solvation of the molecules at the interface

In Fig. 2c, the binding energy splitting ΔE_B is plotted vs. the concentration of pentanol. From low to high concentration a decrease in ΔE_B is observed. In the first region (0 < c < 100 mM), the splitting drops by ≈ 0.21 eV for 1-pentanol (from 1.54 to 1.33 eV) and by ≈ 0.03 eV for 3-pentanol (from 1.36 to 1.33 eV). At ML coverage the two isomers have approximately the same E_B for C_C (≈ 289.87 ± 0.05 eV) and C_{OH} (≈ 291.20 ± 0.05 eV) and thus the same splitting ΔE_B = 1.33 eV. In the second region (c ≥ 100 mM), the splitting decreases further for

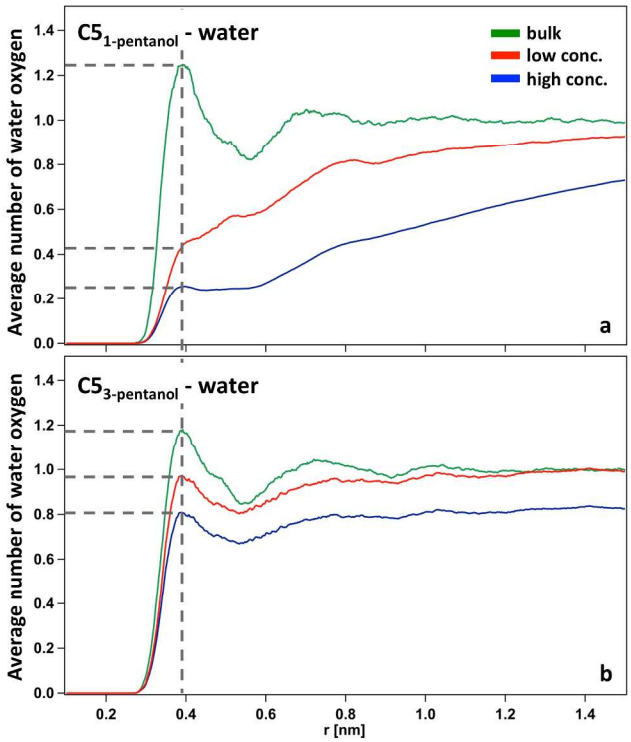

Fig. 4 Results from the MD simulations for the amphiphilic isomers 1-pentanol (a) and 3-pentanol (b) at the aqueous surface. On the y-axis, the average number of water oxygen atoms coordinated around the terminal carbon atom C5 in 1- and 3-pentanol is plotted. On the x-axis the distance from C5 to the surrounding water oxygen atoms is given with 0 being the center of the atom C5.

1-pentanol to 1.26 eV (c = 200 mM), and for 3-pentanol to 1.17 eV (c = 500 mM).

In the first region, up to c_{ML}, interestingly the change in ΔE_B is much larger for 1-pentanol than for 3-pentanol, which almost stays constant. As the chemical shift of the photoelectron's binding energy in these experiments directly reflects the chemical and physical environment of the C_C and C_{OH}, it is clear that in particular for 1-pentanol there is a change in the local molecular environment with concentration.

The initial difference in ΔE_B between 1-pentanol (1.54 eV) and 3-pentanol (1.36 eV) at very low concentration is very similar to the gas phase values (see Fig. 2c), as it originates from inductive effects within the molecules themselves. While in 1-pentanol only one alkyl group is attached to C_{OH}, in 3-pentanol two alkyl groups are attached to it. The replacement of one hydrogen atom by another alkyl group causes an overall higher electron density around C_{OH} resulting in a lower E_B of C_{OH} 1s in 3-pentanol. Assuming a similar E_B of C_C for 1- and 3-pentanol, one thus observes a larger ΔE_B for 1-pentanol.

The change in ΔE_B for 1-pentanol as a function of the concentration is mainly due to a shift in $E_B(C_C)$ to higher binding energies (see Fig. 1). A small shift in $E_B(C_{OH})$ to lower binding energies is observed, however it is in the order of magnitude of the estimated error of 0.05 eV. Thus, the local environment seems to change mainly for C_C with concentration, which is interpreted in terms of desolvation and increasing van der Waals interaction between the alkyl chains as the more polarizable water is exchanged with less polarizable alkyl chains. This causes overall a decrease in screening of the C 1s core-hole, resulting in higher binding energies. The small shift in $E_B(C_{OH})$ of 1-pentanol to lower E_B would be in line with a better screening of the core-hole by neighboring hydroxyl-groups from other alcohols replacing solvating water molecules; however, this remains speculation.

For 3-pentanol, the very small change in ΔE_B is only due to a shift in $E_B(C_C)$ to higher E_B, while $E_B(C_{OH})$ stays constant. That is, the local environment changes only slightly for C_C, while for C_{OH} it does not change as a function of concentration. This indicates that the hydroxyl groups point already towards the water-vapor interface at low concentrations and the alkyl chains are partially solvated (oriented e.g. "parallel" to the water surface), while at higher concentrations they are partially desolvated (pointing rather towards the vacuum), see Fig. 3.

To support our interpretation in terms of a change in the solvation, the MD simulations were evaluated regarding the solvation shell of 1- and 3-pentanol at the interface as a function of concentration. In Fig. 4 the average number of water oxygen atoms surrounding the terminal carbon atom of 1- and 3-pentanol, C5 (see inset in Fig. 1), is plotted versus the radial distance. The simulations were performed using two non-polarizable force fields, GAFF and OPLS/AA, for more details see *Simulations*. Both sets of simulations show the same trend; from low to high concentration the number of water oxygen atoms in the first solvation shell decreases for 1-pentanol, whereas the difference is not at all as large as in the case of 3-pentanol, see Fig. 4. The two force fields used here have been carefully investigated, indicating that for both 1- and 3-pentanol the surface properties should be simulated fairly well.[32] Nevertheless, it is a well-known problem that the interactions between molecules on the surface are not sufficiently strong in non-polarizable force fields.[33,47] This might explain the surprisingly low number of oxygen atoms in the first solvation shell of the terminal carbon atom C5 in the 1-pentanol simulations, see Fig. 4. However, the qualitative agreement between the simulations using the two different force field parameters and the experimental data is a good indicator that the structural changes related to the surface concentration of 1- and 3-pentanol that we see in the simulations give a trustworthy picture of what is observed in the XPS experiment. Here, the shift in the binding energy splitting, which is mainly due to a shift in $E_B(C_C)$ to higher binding energies, was interpreted as being due to desolvation of the alkyl chains and increasing van der Waals interactions.

At concentrations higher than 100 mM, the ΔE_B decreases further, possibly due to the contributing bulk signal. While for low concentrations amphiphiles interact mostly with water in the bulk, at higher concentrations an increase in interaction with other amphiphiles is expected. The structure of the surface-near-bulk region might be pictured with increased interaction between hydrophobic alkyl chains, whereas the hydroxyl groups interact with water.[48] This structure would be in line with the observed shift of $E_B(C_C)$ to higher E_B due to a decrease in screening by water. A possible bilayer formation at the interface of e.g. 3-pentanol, which has been observed for other small amphiphilic molecules at higher concentrations,[49] cannot be completely excluded, however there is neither any indication from the MD simulations nor from the XPS experiments that support this hypothesis.

4 Conclusions

In this study, we investigated the adsorption of two surface-active isomers at the water-vapor interface with surface- and chemically sensitive X-ray photoelectron spectroscopy (XPS)

and molecular dynamics (MD) simulations. As an example for short-chained oxygenated surfactants, which are of relevance in atmospheric science, we focused on the amphiphilic isomers, 1- and 3-pentanol. A concentration-dependent orientation and solvation of the amphiphiles at the aqueous surface is observed. By evaluation of results from C 1s XPS spectra and MD simulations, a deeper understanding of the aqueous surface structure on a molecular level was gained.

At low concentrations the alkyl chains of the two isomers are oriented "parallel" to the aqueous surface while the hydroxyl groups are solvated. The observed difference in binding energy splitting (between C_C and C_{OH}) for the two isomers is interpreted in terms of an inductive effect within the molecules themselves causing a better screening of the final state C_{OH} 1s core-hole in a secondary alcohol (3-pentanol) compared to a primary alcohol (1-pentanol). This difference of electron density distribution within the molecule is in line with a difference in reactivity comparing the two isomers.[50]

At a concentration of approx. 100 mM a monolayer is formed for both isomers, with the molecules being oriented such that the hydroxyl groups point towards the bulk water and the alkyl chains point towards the vapor phase. The ML packing density of 3-pentanol is approx. 70 % of the one observed for 1-pentanol. The molecular area at ≈ 100 mM was calculated to be around 32 ± 2 $Å^2$/molecule for 1-pentanol and around 46 ± 2 $Å^2$/molecule for 3-pentanol, which is equal to a surface concentration of $3.1 \times 10^{+14}$ molecules/cm^2 (1-pentanol) and $2.1 \times 10^{+14}$ molecules/cm^2 (3-pentanol). This difference in packing density could affect both the uptake capability at the water-vapor interface as well as the evaporation from it. At ML coverage, the molar surface concentration is approx. 90 times higher than the bulk concentration for both molecules. For 1-pentanol, a desolvation of the alkyl-groups from low to high concentration is suggested, whereas, for 3-pentanol only a partial desolvation is proposed. This is observed in the XPS experiments as a shift in the binding energy splitting for 1-pentanol (by roughly 0.2 eV), mainly due to a shift in $E_B(C_C)$ to higher binding energies, which is much less pronounced for 3-pentanol. The results from XPS experiments give clear indications about the solvation of the organic molecules at the water-vapor interface, which is strongly supported by MD simulations that enable to quantify the experimentally observed effects.

As mentioned in the introduction, position isomerism is ubiquitous in atmospheric oxidation reactions and it is therefore of interest to understand the impact of different isomers on the surface structure. From our results we see indeed that the effect on the surface structure, such as e.g. surface concentration (molecules/cm^2), is very different for the studied isomers. In general we conclude therefore that isomers – with comparable surface activities – that have smaller molecular areas will be more abundant at the interface in comparison to isomers with larger molecular areas, which might be of crucial importance for the understanding of key properties of aerosols, such as evaporation and uptake capabilities as well as their reactivity.

Acknowledgements

Financial support from the Swedish Research Council (VR), Swedish Foundation for Strategic Research, Helmholtz Association through the Center for Free-Electron Laser Science, Carlsberg Foundation (grants 2009_01_0366 and 2010_01_0391), Finnish Academy of Sciences (257411) and the Carl Tryggers foundation is gratefully acknowledged. MAX IV Laboratory, Lund University, Sweden, is acknowledged for the allocation of beamtime and laboratory facilities. The Swedish National Infrastructure for Computing, UPPMAX is acknowledged for computation.

Notes and references

[a] Uppsala University, Department of Physics and Astronomy, Box 516, 75120 Uppsala, Sweden.
[b] Center for Free-Electron Laser Science, DESY, Notkestrasse 85, 22607 Hamburg, Germany.
[c] Swedish University of Agricultural Sciences, Department of Chemistry and Biotechnology, Box 7015, 75007 Uppsala, Sweden.
[d] Department of Physics, Helsinki University, P.O. Box 64, 00014 Helsinki University, Finland.
[e] MAX IV Laboratory, Lund University, Box 118, 22100 Lund, Sweden.

Electronic Supplementary Information (ESI) available: [Fig. S1: C 1s XPS spectra of 1- and 3-pentanol in aqueous solution. Fig. S2: Evaluation of the aqueous surface thickness from molecular dynamics simulation.]. See DOI: 10.1039/b000000x/

1 K. Valsaraj, *Open J. Phys. Chem.*, 2012, **2**, 58; E. M. Knipping, M. J. Lakin, K. L. Foster, P. Jungwirth, D. J. Tobias, R. B. Gerber, D. Dabdub and F. J. Finlayson-Pitts, *Science*, 2000, **288**, 301.
2 D. Koch and A. D. Del Genio, *Atmos. Chem. Phys*., 2010, **10**, 7685; IPCC, Climate change 2013, The physical science basis, Cambrige University Press (2013), ISBN 978-1-107-66182-0.
3 N. L. Prisle, N. Ottosson, G. Öhrwall, J. Söderström, M. Dal Maso, and O. Björneholm, *Atmos. Chem. Phys.*, 2012, **12**, 12227.
4 T. Novakov and J. Penner, *Nature*, 1993, **365**, 823; J. O. Nriagu and J. M. Pacyna, *Nature*, 1988, **333**, 134.
5 B. Mason, *Nature*, 1954, **174**, 470; D. C. Blanchard, *Science*, 1964, **146**, 396.
6 N. Ottosson, E. Wernersson, J. Söderström, W. Pokapanich, S. Kaufmann, S. Svensson, I. Persson, G. Öhrwall and O. Björneholm, *Phys. Chem. Chem. Phys.*, 2011, **13**, 12261; O. Acevedo and K. Armacost, *J. Am. Chem. Soc.*, 2010, **132**, 1966.
7 N. Ottosson, J. Heyda, E. Wernersson, W. Pokapanich, S. Svensson, B. Winter, G. Öhrwall, P. Jungwirth and O. Björneholm, *Phys. Chem. Chem. Phys.*, 2010, **12**, 10693.
8 N. L. Prisle, T. Raatikainen, A. Laaksonen and M. Bilde, *Atmos. Chem. Phys.*, 2010, **10**, 5663; J. R. Lawrence, S. V. Glass, S.-C. Park and G. M. Nathanson, *J. Phys. Chem. A*, 2005, **109**, 7458.
9 S. V. Glass, S.-C. Park and G. M. Nathanson, *J. Phys. Chem. A*, 2006, **110**, 7593.
10 M. Hallquist. J. C. Wenger, U. Baltensperger, Y. Rudich, D. Simpson, M. Claeys, J. Dommen, N. M. Donahue, C. George, A. H. Goldstein, J. F. Hamilton, H. Herrmann, T. Hoffmann, Y. Iinuma, M. Jang, M. E. Jenkin, J. L. Jimenez, A. Kiendler-Scharr, W. Maenhaut, G. McFiggans, Th. F. Mentel, A. Monod, A. S. H. Prévôt, J. H. Seinfeld, J. D. Surratt, R. Szmigielski and J. Wildt, *Atmos. Chem. Phys.*, 2009, **9**, 5155; P. Artaxo, L. V. Rizzo, J. F. Brito, H. M. J. Barbosa, A. Arana, E. T. Sena, G. G. Cirino, W. Bastos, S. T. Martin and M. O. Andreae, *Faraday Discuss.*, 2013, **165**, 203.
11 H. Singh, Y. Chen, A. Staudt, D. Jacob, D. Blake, B. Heikes and J. Snow, *Nature*, 2001, **410**, 1078.

12 Y.-H. Lin, Z. Zhang, K. S. Docherty, H. Zhang, S. Hapsari Budisulistiorini, C. L. Rubitschun, S. L. Shaw, E. M. Knipping, E. S. Edgerton, T. E. Kleindienst, A. Gold and J. D. Surratt, *Environ. Sci. Technol.*, 2012, **46**, 250; C. R. Ruehl, T. Nah, G. Isaacman, D. R. Worton, A. W. H. Chan, K. R. Kolesar, C. D. Cappa, A. H. Goldstein and K. R. Wilson, *J. Phys. Chem. A*, 2013, **117**, 3990.

13 B. L. J. Poad, H. T. Pham, M. C. Thomas, J. R. Nealon, J. L. Campbell, T. W. Mitchell and S. J. Blanksby, *J. Am. Soc. Mass Spectrom.*, 2010, **21**, 1989; C. Fan, S. Pu, G. Liu and T. Yang, *J. Photochem. Photobio. A*, 2008, **197**, 415.

14 J. Sung, K. Park and D. Kim, *J. Phys. Chem. B*, 2005, **109**, 18507.

15 M. Ehn, J. A. Thornton, E. Kleist, M. Sipilä, H. Junninen, I. Pullinen, M. Springer, F. Rubach, R. Tillmann, B. Lee, F. Lopez-Hilfiker, S. Andres, I.-H. Acir, M. Rissanen, R. Jokinen, S. Schobesberger, J. Kangasluoma, J. Kontkanen, T. Nieminen, T. Kurtén, L. B. Nielsen, S. Jorgensen, H. G. Kjaergaard, M. Canagaratna, M. Dal Maso, T. Berndt, T. Petäjä, A. Wahner, V.-M. Kerminen, M. Kulmala, D. R. Worsnop, J. Wildt and T. F. Mentel, *Nature*, 2014, **506**, 476.

16 P. Lin, A. G. Rincon, M. Kalberer and J. Z. Yu, *Environ. Sci. Technol.*, 2012, **46**, 7454.

17 M. Bässler, A. Ausmees, M. Jurvansuu, R. Feifel, J.O. Forsell, P. de Tarso Fonseca, A. Kivimäki, S. Sundin, S.L. Sorensen, R. Nyholm, O. Björneholm, S. Aksela and S. Svensson, *Nucl. Instr. Meth. Phys. Res. A*, 2001, **469**, 382.

18 B. Winter and M. Faubel, *Chem. Rev.*, 2006, **106**, 1176.

19 S. Hüfner, Photoelectron Spectroscopy, Springer Verlag, Berlin, 1995.

20 B. Winter, R. Weber, W. Widdra, M. Dittmar, M. Faubel and I.V. Hertel, *J. Phys. Chem. A*, 2004, **184**, 2625.

21 R. Stephenson, J. Stuart and M. Tabak, *J. Chem. Eng. Data*, 1984, **29**, 287.

22 N. Preissler, F. Buchner, T. Schultz and A. Lübcke, *J. Phys. Chem. B,* 2013, **117**, 2422.

23 H. Nikjoo, S. Uehara, D. Emfietzoglou and A. Brahme, *New Journal of Physics*, 2008, **10**, 075006; Y.-I. Suzuki, K. Nishizawa, N. Kurahashi, T. Suzuki, *Phys. Rev. E*, 2014, **90**, 010302(R).

24 P. van der Straten, R. Morgenstern and A. Niehaus, *Z. Phys. D*, 1988, **8**, 35.

25 J. L. Campbell and T. Papp, *Atom. Data Nucl. Data Tables*, 2001, **77**, 1.

26 B. Hess, C. Kutzner, D. van der Spoel and E. J. Lindahl, *Chem. Theory Comput.*, 2008, **4**, 435.

27 W. L. Jorgensen and J. Tirado-Rives, *Proc. Natl. Acad. Sci. U. S. A.*, 2005, **102**, 6665; H. J. C. Berendsen, J. R. Grigera and T. P. Straatsma, *J. Phys. Chem.*, 1987, **91**, 6269.

28 W. L. Jorgensen, J. Chandrasekhar, J. D. Madura, R. W. Impey and M. L. Klein, *J. Chem. Phys.*, 1983, **79**, 926.

29 H. J. C. Berendsen, J. P. M. Postma, W. F. van Gunsteren and J. Hermans, Intermolecular Forces, D Reidel Publishing Company, Dordrecht, 1981, 331.

30 J. S. Hub, C. Caleman and D. van der Spoel, *Phys. Chem. Chem. Phys.*, 2012, **14**, 9537.

31 D. van der Spoel, P. J. van Maaren and C. Caleman, *Bioinformatics*, 2012, **28**, 752.

32 C. Caleman, P. J. van Maaren, M. Hong, J. S. Hub, L. T. Costa and D. van der Spoel, *J. Chem. Theory Comput.*, 2012, **8**, 61.

33 E. J. W. Wensink, A. C. Hoffmann, P. J. van Maaren and D. J. van der Spoel, *Chem. Phys.*, 2003, **119**, 7308.

34 D. van der Spoel, P. J. van Maaren, P. Larsson and N. Timneanu, *J. Phys. Chem. B.*, 2006, **110**, 4393.

35 T. Darden, D. York and L. J. Pedersen, *Chem. Phys.*, 1993, **98**, 10089; U. Essmann, L. Perera, M. L. Berkowitz, T. Darden, H. Lee and L. G. J. Pedersen, *Chem. Phys.*, 1995, **103**, 8577.

36 O. F. Lange, D. van der Spoel and B. L. de Groot, *Biophys. J.,* 2010, **99**, 647.

37 H. J. C. Berendsen, J. P. M. Postma, A. Dinola and J. R. Haak, *J. Chem. Phys.*, 1984, **81**, 3684.

38 B. J. Hess, *Chem. Theory Comput.*, 2008, **4**, 116; W. F. van Gunsteren and H. J. C. Berendsen, *Mol. Sim.*, 1988, **1**, 173.

39 N. Ottosson, K. J. Børve, D. Spångberg, L. J. Sæthre, M. Faubel, H. Bergersen, W. Pokapanich, G. Öhrwall, O. Björneholm and B. Winter, *J. Am. Chem. Soc.*, 2011, **133**, 3120.

40 A. W. Adamson and A. P. Gast, Physical Chemistry of Surfaces (sixth ed.) (1997) Wiley, New York.

41 J. Söderström, N. Mårtensson, O. Travnikova, M. Patanen, C. Miron, L. J. Sæthre, K. J. Bœrve, J. J. Rehr, J. J. Kas, F. D. Vila, T. D. Thomas and S. Svensson, *Phys. Rev. Lett.*, 2012, **108**, 193005.

42 K. G. Nath, O. Ivasenko, J. M. MacLeod, J. A. Miwa, J. D. Wuest, A. Nanci, D. F. Perepichka and F. Rosei, *J. Phys. Chem. C*, 2007, **111**, 16996.

43 M. R. Caira, T. le Roex and L. R. Nassimbeni, *Supramol. Chem.*, 2004, **16**, 595.

44 S. Z. Can, D. D. Mago, O. Esenturk and R. Walker, *J. Phys. Chem. C*, 2007, **111**, 8739.

45 J. Werner, J. Julin, M. Dalirian, N. L. Prisle, G. Öhrwall, I. Persson, O. Björneholm and I. Riipinen, *Phys. Chem. Chem. Phys.*, 2014, **39**, 21486.

46 A. Firooz and P. Chen, *J. Colloid Interf. Sci.*, 2012, **370**, 183.

47 B. J. Guillot, *Mol. Liq.*, 2012, **101**, 219.

48 S. Dixit, J. Crain, W. C. K. Poon, J. L. Finney and A. K. Soper, *Nature*, 2002, **416**, 829.

49 E. Tyrode, C. M. Johnson, S. Baldelli, C. Leygraf and M. W. Rutland, *J. Phys. Chem. B*, 2005, **109**, 329; H. Chen, W. Gan, B.-H. Wu, D. Wu, Y. Guo and H.-F. Wang, *J. Phys. Chem. B*, 2005, **109**, 8053; C. M. Johnson, E. Tyrode, A. Kumpulainen and C. Leygraf, *J. Phys. Chem. C*, 2009, **113**, 13209.

50 H. J. Lucas, *J. Am. Chem. Soc.*, 1930, **52**, 802.

Graphical and Textual Abstract for the Contents Pages for Surface Behavior of Amphiphiles in Aqueous Solution: A Comparison between Different Pentanol Isomers

M.-M. Walz[1], C. Caleman[1,2], J. Werner[1,3], V. Ekholm[1], D. Lundberg[3], N. L. Prisle[4], G. Öhrwall[5], and O. Björneholm[1]

Graphical abstract

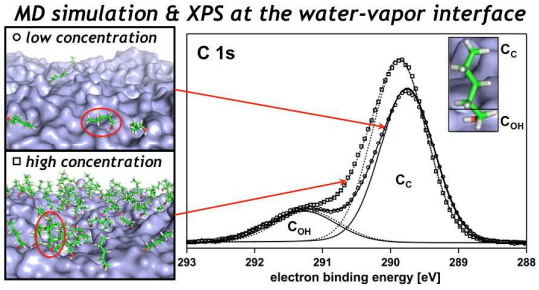

Textual abstract

Molecular-level understanding of concentration-dependent changes in the surface structure of different amphiphilic isomers at the water-vapor interface was gained by molecular dynamics (MD) simulation and X-ray photoelectron spectroscopy (XPS).

[1] *Uppsala University, Department of Physics and Astronomy, Box 516, 75120 Uppsala, Sweden*
[2] *Center for Free-Electron Laser Science, DESY, Notkestrasse 85, 22607 Hamburg, Germany*
[3] *Swedish University of Agricultural Sciences, Department of Chemistry and Biotechnology, Box 7015, 75007 Uppsala, Sweden*
[4] *Department of Physics, Helsinki University, P.O. Box 64, 00014 Helsinki University, Finland*
[5] *MAX-lab, Lund University, Box 118, 22100 Lund, Sweden*